

## Research Article

# Jianpi Qingchang Decoction Ameliorates Chronic Colitis in Piroxicam-Induced IL-10 Knockout Mice by Inhibiting Endoplasmic Reticulum Stress

Qian Chen <sup>1</sup>, Ya-Li Zhang,<sup>1</sup> Zi-Wei Zhang,<sup>1</sup> Yu-Jun Chen,<sup>1</sup> Ying-Jue Tang,<sup>1</sup> Dan Qiao,<sup>1,2</sup> Yan-Cheng Dai <sup>1,2</sup> and Zhi-Peng Tang <sup>1</sup>

<sup>1</sup>Institute of Digestive Disease, Longhua Hospital, Shanghai University of Traditional Chinese Medicine, Shanghai 200032, China

<sup>2</sup>Department of Gastroenterology, Shanghai Traditional Chinese Medicine Integrated Hospital, Shanghai University of Traditional Chinese Medicine, Shanghai 200082, China

Correspondence should be addressed to Yan-Cheng Dai; daiyancheng2005@126.com and Zhi-Peng Tang; zhipengtang@shutcm.edu.cn

Received 18 November 2021; Revised 6 January 2022; Accepted 17 January 2022; Published 9 February 2022

Academic Editor: Lu sa Mota da Silva

Copyright © 2022 Qian Chen et al. This is an open access article distributed under the Creative Commons Attribution License, which permits unrestricted use, distribution, and reproduction in any medium, provided the original work is properly cited.

**Background.** Excessive endoplasmic reticulum (ER) stress in intestinal epithelial cells (IEC) may lead to impaired intestinal mucosal barrier function and then participate in the pathogenesis of ulcerative colitis (UC). Jianpi Qingchang decoction (JPQCD) has been shown to have protective effects on UC. However, further studies are needed to determine whether JPQCD regulates PERK/eIF2 $\alpha$ /ATF4/CHOP pathways to play a role in treating UC. **Methods.** *IL-10*<sup>-/-</sup> mice were randomly assigned into five groups: control, model, low-dose JPQCD (JPQCD L), middle-dose JPQCD (JPQCD M), and high-dose JPQCD (JPQCD H). All groups except for the control group were given model feed containing 200 ppm piroxicam for 10 d to induce colitis. As a comparison, we used wild-type mice that were the progeny of *IL-10*<sup>+/-</sup> matings, bred in the same facility. The control group and wild-type mice were fed with common feed. At the same time, mice in each group were given corresponding drugs by gavage for 14 d. The disease activity index of mice in each group was evaluated daily. Colon tissues of mice were collected, colon length was measured, and pathological changes and ultrastructure of colon epithelial cells were observed. The effects of JPQCD on the PERK/eIF2 $\alpha$ /ATF4/CHOP pathways were evaluated by western blotting and reverse transcription-polymerase chain reaction (RT-PCR). The expression of CHOP in colon tissue was detected by tissue immunofluorescence assay. The expression of NF- $\kappa$ B, p-NF- $\kappa$ B p65 protein was analyzed by western blotting; the level of IL-17 in colon tissue was detected by enzyme-linked immunosorbent assay (ELISA) and verified by examining NF- $\kappa$ B and IL-17 mRNA levels by RT-PCR. **Results.** Compared with the control group, the model group showed significant colitis symptoms and severe colonic tissue damage. The results showed that JPQCD significantly reduced body weight loss, ameliorated disease activity index, and restored colon length in *IL-10*<sup>-/-</sup> mice with piroxicam-induced colitis. Western blotting and RT-PCR showed that the PERK/eIF2 $\alpha$ /ATF4/CHOP pathway was activated in colon tissue of model mice, suggesting that the pathway is involved in the pathogenesis of ulcerative colitis (UC) and could become a potential therapeutic target. The JPQCD treatment inhibited the activation of the PERK/eIF2 $\alpha$ /ATF4/CHOP pathway, alleviated the ER stress, and played a role in preventing and treating UC. In addition, JPQCD can also downregulate the protein of NF- $\kappa$ B, p-NF- $\kappa$ B p65, downregulate the mRNA expression of NF- $\kappa$ B, and reduce the content of IL-17 and its mRNA expression in colon tissues. **Conclusion.** JPQCD may play a protective role in UC by regulating the PERK/eIF2 $\alpha$ /ATF4/CHOP signaling pathway and relieving endoplasmic reticulum stress.

## 1. Introduction

Ulcerative colitis (UC) is a chronic nonspecific intestinal inflammatory disease characterized by continuous and diffuse inflammatory changes in the colorectal mucosa. Its lesions are mainly confined to the large intestinal mucosa and submucosa. Clinical manifestations are diarrhea, mucous pus and blood in the stools, and abdominal pain. The severity of the disease varies, and most cases show a chronic course of recurrent attacks [1]. The incidence and prevalence of UC are increasing worldwide. The etiology of UC is not clear, and it is generally considered to be related to factors such as heredity, environment, intestinal microecology, and immune imbalance [2]. So far, aminosalicylic acid preparations, corticosteroids, and immunosuppressants are the main drugs for the treatment of UC. However, these drugs are accompanied by a variety of potential adverse effects [3]. As an alternative and complementary medicine for the treatment of inflammatory bowel disease (IBD), traditional Chinese medicine (TCM) has unique advantages for the prevention and treatment of IBD due to its efficacy and safety [4, 5].

It has been shown that various causes contribute to intestinal epithelial cell (IEC) endoplasmic reticulum (ER) stress and activate the unfolded protein response (UPR), which collectively participate in the development of IBD [6, 7]. UPR is controlled by three major sensors: pancreatic ER eIF2 $\alpha$  kinase (PERK), inositol-requiring enzyme 1 (IRE1), and activating transcription factor 6 (ATF6) [8]. In the absence of ER stress, glucose-regulated protein 78 (GRP78) binds to the luminal domains of the ER stress sensors and is maintained in an inactive state [9]. Upon ER stress, GRP78 dissociates from three proteins, thus activating PERK, IRE1, or ATF6 and starting UPR, thus promoting the correct folding of proteins and inhibiting the synthesis of proteins [10]. Among the three pathways of ER stress, the PERK pathway mainly recognizes and interacts with a variety of unfolded proteins to regulate protein synthesis [11].

Jianpi Qingchang decoction (JPQCD) is composed of *Coptis chinensis* Franch. (Huang Lian) 3 g, *Astragalus mongholicus* Bunge (Huang Qi) 30 g, *Codonopsis pilosula* (Franch.) Nannf. (Dang Shen) 15 g, *Portulaca oleracea* L. (Ma Chi Xian) 30 g, *Sanguisorba officinalis* L. (Sheng Di Yu) 15 g, *Panax notoginseng* (Burkill) F. H. Chen (San Qi) 6 g, *Bletilla striata* (Thunb.) Rchb.f. (Bai Ji) 3 g, *Aucklandia costus* Falc. (Mu Xiang) 6 g, and *Glycyrrhiza uralensis* Fisch. ex DC. (Gan Cao) 6 g. Previous studies have shown that JPQCD can significantly alleviate the clinical symptoms of patients with mild-to-moderate active UC and thus improve their quality of life [12]. Previous experimental studies have shown that JPQCD can significantly improve the symptoms of dextran sodium sulfate- (DSS-) induced colitis, and the mechanism may be related to the inhibition of nuclear factor- (NF-)  $\kappa$ B activation, downregulation of inflammatory mediators such as interleukin- (IL-) 1 $\beta$ , IL-8, tumor necrosis factor- $\alpha$ , and improvement of colonic epithelial barrier function in mice [13, 14]. Moreover, we found that JPQCD can also regulate DSS-induced abnormal intestinal motility

in UC mice by inhibiting intestinal inflammatory cascading and reducing autophagy of Cajal stromal cells [15]. However, it is not clear whether JPQCD can regulate the PERK/eIF2 $\alpha$ /ATF4/CHOP pathway. In this study, we used piroxicam to induce *IL-10*<sup>-/-</sup> mice to produce a chronic colitis model and explored whether JPQCD could regulate the PERK/eIF2 $\alpha$ /ATF4/CHOP pathway, thus improving ER stress and preventing UC.

## 2. Materials and Methods

**2.1. Animals and Experimental Design.** *IL-10*<sup>-/-</sup> mice on a C57BL/6 strain background were obtained from Shanghai Model Organisms (license No. SCXK (Shanghai) 2017-0010). Mice were bred and mated in SPF Animal Experimental Center of Shanghai University of Traditional Chinese Medicine (license No. SCXK (Shanghai) 2020-0009), under standard conditions (room temperature, 24  $\pm$  2°C; humidity 50%–60%; 12 h light/dark cycle). Shanghai Model Organisms provided genetic testing services. This study was reviewed and approved by the Experimental Animal Ethics Committee of Shanghai University of Chinese Medicine (PZSHUTCM190912020).

Using SPSS version 25.0 to generate random numbers, *IL-10*<sup>-/-</sup> mice were randomly assigned to five groups: control, model, low-dose JPQCD (JPQCD L), middle-dose JPQCD (JPQCD M), and high-dose JPQCD (JPQCD H) ( $n=8$ , 4 male and 4 female). Chow containing piroxicam (Sigma–Aldrich, St. Louis, MO, USA) was fed to *IL-10*<sup>-/-</sup> mice for 10 d at a dose of 200 ppm to induce colitis [16]. For comparison, we used wild-type mice that were the progeny of *IL-10*<sup>+/-</sup> matings, bred in the same facility. Control and wild-type mice were fed a common diet. Mice in the treatment group were given JPQCD (10, 15, or 22.5 g/kg/d) by gavage for 2 wk, and mice in the model group, control group, and wild-type group were given normal saline by gavage. The animal experiment was conducted in accordance with the Laboratory Animal Regulations of the Institutional Animal Care and Use Committee of Shanghai University of Traditional Chinese Medicine and was approved by the Institutional Animal Care and Use Committee of Shanghai University of Traditional Chinese Medicine. During the experiment, the body weight, stool characteristics, and fecal occult blood of mice in each group were recorded every day. The disease activity index (DAI) refers to Sánchez's method and is described in Table 1, which is composed of the mean value of the sum of the three indexes [17].

**2.2. Preparation of JPQCD.** The nine medicinal herbs contained in JPQCD (listed above) were purchased from Longhua Hospital Shanghai University of Traditional Chinese Medicine (Shanghai, China). After soaking the above medicines, they were decocted twice, filtered, and concentrated to a volume of 600 mL. After being concentrated in a rotary evaporator, the concentrated JPQCD was placed in a freeze-drying machine to prepare freeze-dried powder, which was sealed and stored at -20°C.

TABLE 1: Disease activity index score.

Weight loss(%)	Stool consistency	Bleeding	Score
0	Normal pellets	Normal	0
1~5	Loose feces	Occult blood positive	1
6~10			2
11~15	Watery diarrhea	Visible bleeding	3
>16			4

**2.3. Ultrapformance Liquid Chromatography Quadrupole-Time of Flight Mass Spectrometer (UPLC-Q-TOF/MS).** Accurately weigh 0.5 g of JPQCD powder into a 50 mL stoppered conical flask and add 25 ml of 80% methanol solution, ultrasonicated for 30 min, cooled to room temperature, centrifuged at 12000 rpm for 5 min, and the supernatant was taken for detection.

Chemical profiling of JPQCD was performed on an Agilent 1290 UPLC System (Agilent Technologies, Palo Alto, USA) coupled with Sciex Triple TOF® 4600 high-resolution mass spectrum (AB Sciex, Darmstadt, Germany). Chromatographic column using Agilent ZORBAX RRHD Eclipse XDB-C18 (2.1 × 100 mm, 1.8 μm). The mobile phase consisted of water containing 0.1% formic acid (A) and acetonitrile (B). The following gradient condition was used: 0–5 min, 5%–5% B; 5–7 min, 5%–10% B; 7–23 min 10%–15% B; 23–36 min, 15%–30% B; 36–48 min, 30%–50% B; 48–50 min, 50%–95% B; 50–52 min, 95%–95% B; 52–52.1 min, 95%–5% B; 52.1–54 min, 5%–5% B. Column oven temperature was set at 30°C, while the flow rate was 0.3 mL/min. Mass spectrometry detection mode is electrospray ionization (ESI) source negative/positive ion mode.

**2.4. Histological Analysis.** Colon tissue from the anus to the ileocecal part of mice was cut and colon length was measured with a ruler. The distal colon was collected 1 cm from the anus and about 0.5 cm in length for histopathological analysis. Colon tissue was fixed with 10% neutral formalin buffer solution, washed for 4 h under running water, embedded in paraffin, and stained with hematoxylin and eosin (H&E). The specific steps were as follows: dehydration with graded ethanol, Xylene, and wax immersion, embedding in paraffin; cutting into 4 μm sections, baking at 60°C for 1 h, H&E staining, sealing with neutral gum, observing under a microscope, and taking pictures.

**2.5. Transmission Electron Microscopy.** The fresh colon tissue was cut into 1-mm<sup>3</sup> pieces, fixed in 2.5% glutaraldehyde for 2 h, and fixed in 1% osmium at 4°C for 3 h. The tissue was dehydrated with graded ethanol and acetone, and embedded and cured. Ultrathin sections were cut with a thickness of 50–60 nm, and double-stained with 3% uranyl acetate and lead citrate. The ultrastructure of the ER in colonic epithelial cells was observed by transmission electron microscopy.

**2.6. RNA Isolation and Quantitative Reverse Transcription-Polymerase Chain Reaction (RT-PCR).** Total RNA was extracted from colon tissue using TRIzol (Invitrogen, Carlsbad, CA, USA) and the concentration was determined.

The extracted RNA was reverse transcribed to cDNA using a reverse transcription kit (Takara, Kyoto, Japan) and RT-PCR was conducted based on the Eppendorf PCR system. The mRNA expression of the following genes was assessed using qPCR: *β-actin*, *PERK*, *eIF2α*, *GRP78*, *ATF4*, *CHOP*, *NF-κB*, *IL-17*. The relative expression of target genes was calculated using the  $\Delta\Delta C_t$  method. Primer sequences are presented in Table 2.

**2.7. Western Blotting.** Frozen colon tissue samples were homogenized in lysis buffer to obtain total protein. Protein concentration was determined in supernatants using the BCA Protein concentration determination kit (Beyotime, Shanghai, China). Equal amounts of protein were separated by SDS-PAGE and transferred to the polyvinylidene difluoride membrane. The membranes were blocked in 5% nonfat milk for 1 h, and membranes were incubated at 4°C overnight with primary antibodies to p-PERK, eIF2α, p-eIF2α, CHOP, NF-κB, β-actin (from Cell Signaling, Danvers, MA, USA), GRP78 (from Proteintech, Wuhan, Hubei, China), ATF4 (from Santa Cruz, Dallas, TX, USA), and p-NF-κB p65 (from ABclonal, Wuhan, Hubei, China). The membranes were incubated with secondary antibodies, anti-rabbit IgG or anti-mouse IgG (from Cell Signaling, Danvers, MA, USA) for 1 h at room temperature. Protein bands were quantified using ImageJ and the grey value of the targets was normalized by β-actin.

**2.8. Immunofluorescence.** To investigate localization of CHOP, paraffin sections of the colon were dewaxed to water, antigen repaired, blocked, and then incubated with CHOP (1 : 400) overnight. The secondary antibody was incubated at room temperature for 1 h and then stained with DAPI for 2 min.

**2.9. Enzyme-Linked Immunosorbent Assay.** The colon tissue of 50 mg mice was weighed and added 1 mL of precooled PBS. After homogenization, the supernatant was centrifuged at 5000x g for 5 min. Experiments were done following the instructions of the Mouse IL-17 ELISA kit (from Elabscience, Wuhan, Hubei, China).

**2.10. Statistical Analysis.** All data are presented as mean ± SEM. Statistical differences between different groups were measured through one-way ANOVA. Results were considered statistically significant at  $P < 0.05$ . Data analyses were conducted using SPSS version 25.0.

### 3. Results

**3.1. Phytochemicals Identification of JPQCD.** Forty-four phytochemicals in JPQCD were identified by UPLC-Q-TOF/MS-based on multistage mass spectrum information of samples, high-resolution mass spectrum database of natural products, and relevant literature (Table 3). Among them, 9 compounds were from *Glycyrrhiza uralensis* Fisch. ex DC., 8 compounds from *Sanguisorba officinalis* L., and 8

TABLE 2: List of primers used in this study.

Gene		Primer sequence
GRP78	Forward	TTGTCCCCTTACACTTGGTATTG
	Reverse	TGTCCTTTTGTAGGGGTCGTTTC
PERK	Forward	GCTCAAAGACGAAAGCACAGAC
	Reverse	CCCACCGAGAAAGACCGAC
eIF2 $\alpha$	Forward	ACCTGGATACGGTGCCCTACG
	Reverse	TCGAATTTTGACCGCTTGTG
ATF4	Forward	ATGGAGCAAACAAGACAGCA
	Reverse	TGCCTTACGGACCTCTCTATC
CHOP	Forward	AAACCTTCACTACTCTTGACCCTG
	Reverse	GGGCACTGACCACTCTGTTTC
$\beta$ -actin	Forward	GAGACCTTCAACACCCAGC
	Reverse	ATGTCACGCACGATTTCCC

compounds from *Panax notoginseng* (Burkill) F. H. Chen. Five compounds are derived from *Bletilla striata* (Thunb.) Rchb.f.. Then, there were 4, 3, 3, 2, and 1 compounds derived from *Coptis chinensis* Franch., *Portulaca oleracea* L., *Astragalus mongholicus* Bunge, *Aucklandia costus* Falc., and *Codonopsis pilosula* (Franch.) Nannf. The UPLC-Q-TOF/MS chromatographic profile is shown in Figure 1.

**3.2. JPQCD Alleviated the Symptoms of Experimental Chronic Colitis in  $IL-10^{-/-}$  Mice.** We established a mouse model of chronic colitis by adding 200 ppm piroxicam feed to  $IL-10^{-/-}$  mice for 10 d to evaluate the therapeutic effect of JPQCD (Figure 2(a)).  $IL-10^{-/-}$  mice exposed to piroxicam showed significant weight loss, diarrhea, and blood in the stools. DAI of mice in the model group was higher than that in the wild-type group and control group, and JPQCD treatment significantly increased body weight and reduced DAI (Figures 2(b) and 2(c)). Colonic shortening indirectly reflected the pathological process of colitis, and JPQCD significantly alleviated piroxicam-induced colonic shortening in mice (Figure 2(d)).

**3.3. JPQCD Inhibited Intestinal Inflammatory Infiltration of Experimental Chronic Colitis in  $IL-10^{-/-}$  Mice.** H&E staining showed that the colon crypts of wild-type mice were normal, with abundant goblet cells, few lamina propria monocytes, and no sign of mucosal thickening or ulceration. In the model group, there was a lot of inflammatory cell infiltration, mucosal thickening, goblet cell reduction, obvious ulceration, and irregular glandular arrangement in the colonic tissues. The JPQCD-treated mice showed intact colonic structures, no obvious ulcers, and less inflammatory cell infiltration (Figures 3(a)–3(f)).

**3.4. JPQCD Reduced ER Stress in IECs of Mice with Piroxicam-Induced Colitis.** The colonic epithelial cells were observed under transmission electron microscopy. In the wild-type and control groups, the ER showed a membranous network structure, clear and in clumps; the omental cavity was not expanded, and a large number of ribosomes were attached to it; and the cells had many mitochondria with a light color. In the model group, the rough ER (RER) was increased, and the ER cavity was significantly expanded. There were many ER

cavities of different sizes and shapes, which were vacuolated and partially fused into clusters. In the JPQCD group, the RER was reduced compared with that in the model group and slightly dilated with less quantity, and the morphology tended to be reticular. In conclusion, JPQCD improved ER stress in IECs of mice with colitis (Figures 4(a)–4(f)).

**3.5. JPQCD Regulated Gene Expression Related to PERK/eIF2 $\alpha$ /ATF4/CHOP Signaling Pathway.** To further investigate the effect of JPQCD on piroxicam-induced colitis, we performed an RT-PCR analysis of several signaling molecules. Compared with the control group, the mRNA levels of PERK, eIF2 $\alpha$ , GRP78, ATF4, and CHOP in the model group were higher. The mRNA expression of PERK, eIF2 $\alpha$ , GRP78, ATF4, and CHOP in the colon of the JPQCD group was significantly lower than that in the model group. These results suggested that JPQCD-induced improvement in experimental colitis in mice was associated with the PERK/eIF2 $\alpha$ /ATF4/CHOP signaling pathway (Figures 5(a)–5(f)).

**3.6. JPQCD Regulated Expression of Proteins Related to the PERK/eIF2 $\alpha$ /ATF4/CHOP Signaling Pathway.** To further investigate the anti-inflammatory mechanism of JPQCD, we detected the protein expression of key signaling molecules in the PERK/eIF2 $\alpha$ /ATF4/CHOP pathway. Western blotting showed that PERK, eIF2 $\alpha$ , GRP78, ATF4, and CHOP proteins were highly expressed in the model group, while JPQCD treatment significantly reduced the expression of these proteins. The results showed that the improvement of experimental colitis symptoms in mice induced by JPQCD was associated with inhibition of the PERK/eIF2 $\alpha$ /ATF4/CHOP signaling pathway (Figures 6(a)–6(f)). Immunofluorescence staining further confirmed that JPQCD could depress CHOP expression in piroxicam-induced colitis mice (Figure 6(g)).

**3.7. JPQCD Inhibited the Activation of NF- $\kappa$ B and IL-17.** NF- $\kappa$ B is considered to be the key molecular pathway of UC. We detected the effects of JPQCD on the expression of NF- $\kappa$ B by Western blot. The expression of NF- $\kappa$ B protein increased significantly in the colon of piroxicam-induced colitis, which was inhibited by JPQCD treatment (Figure 7(a)). The protein level of p-NF- $\kappa$ B p65 reflected its transcription in the nucleus, and JPQCD significantly inhibited the phosphorylation level of p65 (Figure 7(b)). Since IL-17 is a cytokine with a strong proinflammatory activity involved in the pathogenesis of a variety of chronic inflammatory diseases, we used ELISA to detect the level of IL-17 in colonic tissues. A significant elevation of IL-17 content was observed in model mice compared with the control mice. The elevated IL-17 level was significantly decreased in colitis mice treated with JPQCD (Figure 7(c)). To further verify the inhibitory effects of JPQCD on NF- $\kappa$ B and IL-17, we determined the mRNA levels of NF- $\kappa$ B and IL-17 in the colon by RT-PCR. The results showed that the mRNA expressions of NF- $\kappa$ B and IL-17 in the JPQCD group were significantly lower than those in the model group

TABLE 3: Identification results of main components of JPQCD.

NO	Retention time (min)	Adducts	Measured M/Z	Expected M/Z	ppm	Formula	Molecular weight	Phytochemical name	MS/MS spectra
1	1.81	[M-H] <sup>-</sup>	169.0158	169.0142	9.2	C <sub>7</sub> H <sub>6</sub> O <sub>5</sub>	170.02	Gallic acid	169.0168; 125.0250; 81.0368
2	5.29	[M-H] <sup>-</sup>	345.0832	345.0827	1.4	C <sub>14</sub> H <sub>18</sub> O <sub>10</sub>	346.09	Methyl 6-O-galloyl-β-D-glucoside	345.0814; 313.0536; 124.0170 289.0721; 271.0594; 245.0833; 203.0725; 151.0401 277.0032; 197.0455; 182.0225; 166.9997; 123.0086 289.0737; 245.0844; 203.0715;
3	9.15	[M-H] <sup>-</sup>	289.0737	289.0718	6.7	C <sub>15</sub> H <sub>14</sub> O <sub>6</sub>	290.08	Catechin	151.0419 511.2700; 465.2368; 333.1949; 311.0997; 251.0743 417.1190; 255.0670; 135.0101; 119.0510
4	11.26	[M-H] <sup>-</sup>	277.0034	277.0024	3.7	C <sub>9</sub> H <sub>10</sub> O <sub>8</sub> S	278.01	Gallic acid ethyl ester sulfate	285.0746; 270.0507 619.2267; 439.1630; 171.0665; 153.0568 549.1600; 255.0650; 135.0084 342.0961;
5	12.54	[M-H] <sup>-</sup>	289.0735	289.0718	6.0	C <sub>15</sub> H <sub>14</sub> O <sub>6</sub>	290.08	Epicatechin	147.0431; 85.0268
6	18.78	[M+FA-H] <sup>-</sup>	511.2434	511.2396	7.4	C <sub>21</sub> H <sub>38</sub> O <sub>11</sub>	466.24	Rhodiolide E	372.1090; 177.0529; 145.0260 457.1745; 285.0957; 189.0746; 171.0664; 153.0556 457.1737; 285.0976; 153.0576; 127.0770 320.0907; 292.0961; 277.0757; 249.0733 887.3237; 619.2214; 439.1595; 179.0563
7	20.40	[M-H] <sup>-</sup>	417.1220	417.1191	6.9	C <sub>21</sub> H <sub>22</sub> O <sub>9</sub>	418.13	Liquiritin	
8	20.41	[M+H] <sup>+</sup>	447.1256	447.1286	-6.7	C <sub>22</sub> H <sub>22</sub> O <sub>10</sub>	446.12	Calycosin-7-O-β-D-glucoside	
9	21.52	[M-H] <sup>-</sup>	619.2303	619.2244	9.6	C <sub>27</sub> H <sub>40</sub> O <sub>16</sub>	620.23	Dactylorhin E	
10	21.57	[M-H] <sup>-</sup>	549.1631	549.1614	3.2	C <sub>26</sub> H <sub>30</sub> O <sub>13</sub>	550.17	Liquiritin apioside	
11	22.16	[M+H] <sup>+</sup>	504.1466	504.15	-6.8	C <sub>24</sub> H <sub>25</sub> NO <sub>11</sub>	503.14	Oleracein A	
12	24.67	[M+H] <sup>+</sup>	534.159	534.1606	-3	C <sub>25</sub> H <sub>27</sub> NO <sub>12</sub>	533.15	Oleracein B	
13	27.62	[M-H] <sup>-</sup>	457.1737	457.1715	4.7	C <sub>21</sub> H <sub>30</sub> O <sub>11</sub>	458.18	Gymnoside II	
14	28.37	[M-H] <sup>-</sup>	457.1753	457.1715	8.2	C <sub>21</sub> H <sub>30</sub> O <sub>11</sub>	458.18	Gymnoside I	
15	28.55	M <sup>+</sup>	320.0897	320.0917	-6.4	C <sub>19</sub> H <sub>14</sub> NO <sub>4</sub>	320.09	Coptisine	
16	28.76	[M+FA-H] <sup>-</sup>	933.3300	933.3245	5.9	C <sub>40</sub> H <sub>56</sub> O <sub>22</sub>	888.33	Dactylorhin A	

TABLE 3: Continued.

NO	Retention time (min)	Adducts	Measured M/Z	Expected M/Z	ppm	Formula	Molecular weight	Phytochemical name	MS/MS spectra
17	29.04	M <sup>+</sup>	338.1364	338.1387	-6.8	C <sub>20</sub> H <sub>20</sub> NO <sub>4</sub>	338.14	Jatrorrhizine	338.1386; 322.1051; 208.0897; 294.1110; 279.0878 305.1232;
18	29.22	[M + FA - H] <sup>-</sup>	441.1797	441.1766	7.0	C <sub>20</sub> H <sub>28</sub> O <sub>8</sub>	396.18	Lobetyolin	215.1090; 185.0984; 159.0830; 143.0720 267.0671;
19	30.81	[M + FA - H] <sup>-</sup>	475.1273	475.1246	5.7	C <sub>22</sub> H <sub>22</sub> O <sub>9</sub>	430.13	Ononin	252.0399; 223.0389 549.1654;
20	30.96	[M - H] <sup>-</sup>	549.1657	549.1614	7.9	C <sub>26</sub> H <sub>30</sub> O <sub>13</sub>	550.17	Isoliquiritin apioside	255.0655; 135.0104 977.5391;
21	31.72	[M + FA - H] <sup>-</sup>	977.5402	977.5327	7.7	C <sub>47</sub> H <sub>80</sub> O <sub>18</sub>	932.53	Notoginsenoside R1	931.5254; 799.4847; 637.4346 314.1417;
22	32.16	[M + H] <sup>+</sup>	314.1388	314.1387	0.4	C <sub>18</sub> H <sub>19</sub> NO <sub>4</sub>	313.13	N-trans-Feruloyltyramine	177.0538; 145.0276; 121.0637 352.1538;
23	32.34	M <sup>+</sup>	352.1528	352.1543	-4.4	C <sub>21</sub> H <sub>22</sub> NO <sub>4</sub>	352.15	Palmatine	336.1192; 322.1032; 308.1216; 294.1076 336.1213;
24	32.44	M <sup>+</sup>	336.1216	336.1230	-4.3	C <sub>20</sub> H <sub>18</sub> NO <sub>4</sub>	336.13	Berberine	320.0906; 292.0947; 276.1035 725.2715;
25	32.69	[M + FA - H] <sup>-</sup>	771.2747	771.2717	3.9	C <sub>34</sub> H <sub>46</sub> O <sub>17</sub>	726.27	Militarine	457.1722; 285.0982; 153.0566 845.4965;
26	32.83	[M + FA - H] <sup>-</sup>	845.4934	845.4904	3.5	C <sub>42</sub> H <sub>72</sub> O <sub>14</sub>	800.49	Ginsenoside Rg1	799.4888; 637.4343; 475.3814 329.0298;
27	33.16	[M - H] <sup>-</sup>	408.9890	408.9871	4.6	C <sub>16</sub> H <sub>10</sub> O <sub>11</sub> S	409.99	3,3'-Di-O-methylelagic acid sulfate	314.0055; 298.9820; 286.0127 493.2369;
28	34.34	[M + FA - H] <sup>-</sup>	493.2308	493.2291	3.5	C <sub>21</sub> H <sub>36</sub> O <sub>10</sub>	448.23	Geraniol 1-O- $\alpha$ -L-arabinofuranosyl-(1 $\rightarrow$ 6)- $\beta$ -D-glucopyranoside	447.2270; 315.1806; 221.0679; 179.0579 423.0065;
29	35.30	[M - H] <sup>-</sup>	423.0051	423.0028	5.5	C <sub>17</sub> H <sub>12</sub> O <sub>11</sub> S	424.01	2,3,8-Tri-O-methylelagic acid sulfate	343.0475; 328.0216; 312.9979; 297.9731 983.4449;
30	38.58	[M - H] <sup>-</sup>	983.4580	983.4493	8.8	C <sub>48</sub> H <sub>72</sub> O <sub>21</sub>	984.46	Licorice saponin A3	821.3791

TABLE 3: Continued.

NO	Retention time (min)	Adducts	Measured M/Z	Expected M/Z	ppm	Formula	Molecular weight	Phytochemical name	MS/MS spectra
31	39.35	[M + FA-H] <sup>-</sup>	815.4855	815.4798	6.9	C <sub>41</sub> H <sub>70</sub> O <sub>13</sub>	770.48	Ginsenoside F3	815.4920; 769.4752; 637.4285; 475.3756 837.3894;
32	39.79	[M-H] <sup>-</sup>	837.3954	837.3914	4.7	C <sub>42</sub> H <sub>62</sub> O <sub>17</sub>	838.40	Licoricesaponin G2	351.0538; 193.0391 683.4435;
33	40.40	[M + FA-H] <sup>-</sup>	683.4427	683.4376	7.5	C <sub>36</sub> H <sub>62</sub> O <sub>9</sub>	638.44	Ginsenoside Rh1	637.4295; 475.3811 1153.6143;
34	40.50	[M + FA-H] <sup>-</sup>	1153.6127	1153.6011	10.0	C <sub>54</sub> H <sub>92</sub> O <sub>23</sub>	1108.60	Ginsenoside Rb1	1107.5910; 945.5482 811.4522;
35	40.62	[M + FA-H] <sup>-</sup>	811.4566	811.4485	9.9	C <sub>41</sub> H <sub>66</sub> O <sub>13</sub>	766.45	Ziyuglycoside I	765.4467; 603.3907; 207.0512 683.4427;
36	40.88	[M + FA-H] <sup>-</sup>	683.4404	683.4376	4.1	C <sub>36</sub> H <sub>62</sub> O <sub>9</sub>	638.44	Ginsenoside F1	637.4368; 475.3848 837.3965;
37	41.46	[M-H] <sup>-</sup>	837.3983	837.3914	8.2	C <sub>42</sub> H <sub>62</sub> O <sub>17</sub>	838.40	Licoricesaponin Q2	351.0573 829.4714;
38	41.99	[M + FA-H] <sup>-</sup>	829.4671	829.4591	9.6	C <sub>41</sub> H <sub>68</sub> O <sub>14</sub>	784.46	Astragaloside A	783.4561; 489.3715 991.5596;
39	42.95	[M + FA-H] <sup>-</sup>	991.5574	991.5483	9.2	C <sub>48</sub> H <sub>82</sub> O <sub>18</sub>	946.55	Ginsenoside Rd	945.5476; 783.5021; 621.4569 821.3926;
40	43.09	[M-H] <sup>-</sup>	821.4006	821.3965	5.0	C <sub>42</sub> H <sub>62</sub> O <sub>16</sub>	822.40	Glycyrrhizic acid	351.0580 821.3966;
41	44.57	[M-H] <sup>-</sup>	821.4037	821.3965	8.8	C <sub>42</sub> H <sub>62</sub> O <sub>16</sub>	822.40	Uralsaponin B	351.0582 829.5000;
42	49.14	[M + FA-H] <sup>-</sup>	829.5022	829.4955	8.1	C <sub>42</sub> H <sub>72</sub> O <sub>13</sub>	784.50	Ginsenoside Rg3	783.4923; 621.4401 231.1381;
43	50.43	[M + H] <sup>+</sup>	231.1365	231.138	-6.3	C <sub>15</sub> H <sub>18</sub> O <sub>2</sub>	232.15	Dehydrocostus Lactone	185.1323; 165.0682; 128.0604; 105.0691 231.1407;
44	50.78	[M-H] <sup>-</sup>	231.1411	231.1391	8.9	C <sub>15</sub> H <sub>20</sub> O <sub>2</sub>	232.15	Costunolide	213.1291

(Figure 7(d)). In summary, these data indicate that JPQCD can reduce the inflammatory response by alleviating endoplasmic reticulum stress and regulating the PERK/eIF2 $\alpha$ /ATF4/CHOP signaling pathway, with the specific mechanism shown in Figure 8.

#### 4. Discussion

UC is a chronic recurrent intestinal inflammatory disease classified as one of the refractory diseases by the World Health Organization. Due to the many adverse effects of current therapies, it is urgent to find an effective and safe treatment method for UC. The purpose of this study was to investigate the efficacy and potential mechanism of JPQCD

in reducing piroxicam-induced chronic colitis in *IL-10*<sup>-/-</sup> mice. We found that JPQCD repaired the intestinal mucosal barrier in mice, significantly reduced the piroxicam-induced colon inflammatory response, alleviated ER stress of colonic epithelial cells, and regulated the PERK/eIF2 $\alpha$ /ATF4/CHOP pathway.

In our study, we used a chronic colitis model of *IL-10*<sup>-/-</sup> mice induced by piroxicam. The *IL-10*<sup>-/-</sup> mice is a genetic engineering model widely used for analyzing the causes of inflammatory bowel disease, which was established by Kühn et al. in 1993 [18]. In previous studies, we have demonstrated the efficacy of JPQCD in DSS-induced colitis in mice [13–15]. However, the use of chemical reagents to damage the colonic mucosal barrier of mice, increase its

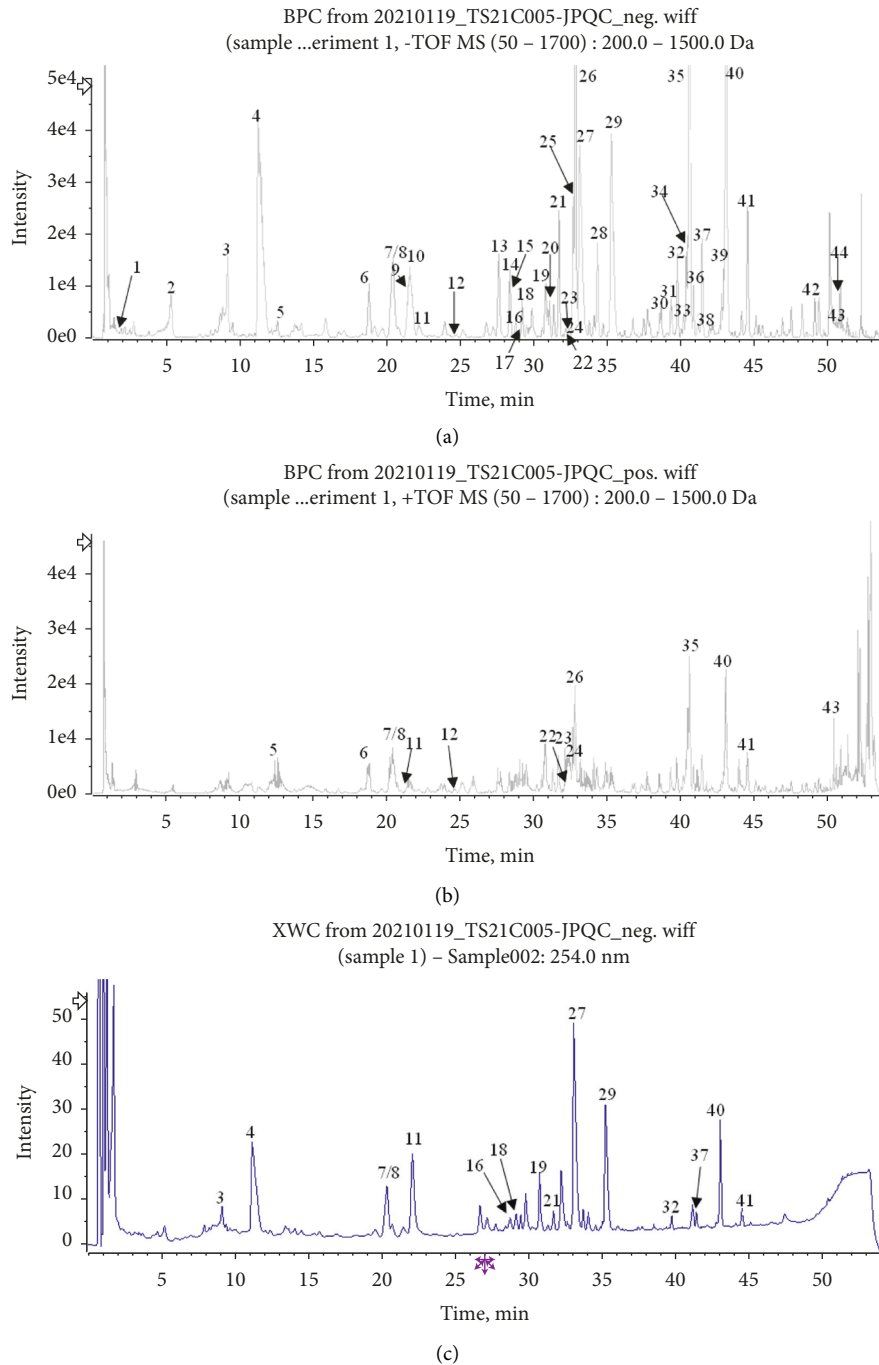


FIGURE 1: UPLC-Q-TOF/MS of JPQCD. (a) UPLC-HRMS base peak ion flow graph (BPC) negative ion mode for JPQCD; (b) UPLC-HRMS BPC-positive ion mode for JPQCD; (c) UPLC UV chromatogram of JPQCD-UV 254 nm.

permeability, and then trigger the production of inflammatory lesions in the intestinal tract is significantly different from the mechanism of inflammatory bowel disease induced by diet, immunity, infection, spirit, and other factors in human UC, which limits the experimental research. The use of gene knockout technology to replicate animal models of UC has the characteristics of spontaneity and can simulate human UC, which is important for revealing the etiology, clarifying the genetic pathogenesis of the disease, and determining susceptibility genes [19]. It has been shown that,

in C57BL/6  $IL-10^{-/-}$  mice, spontaneous colitis development is slow, and the use of nonsteroidal anti-inflammatory drugs (NSAIDs) such as piroxicam can induce moderately severe colitis in 2 wk. Acute symptoms turned chronic after withdrawal of the drug, and its pathological features were consistent with those observed in the colonic tissues of spontaneous colitis mice, while wild-type mice exposed to NSAIDs did not develop colitis [20, 21]. The histopathological characteristics of  $IL-10^{-/-}$  mouse colitis are similar to those of human IBD, including lamellar and submucosal

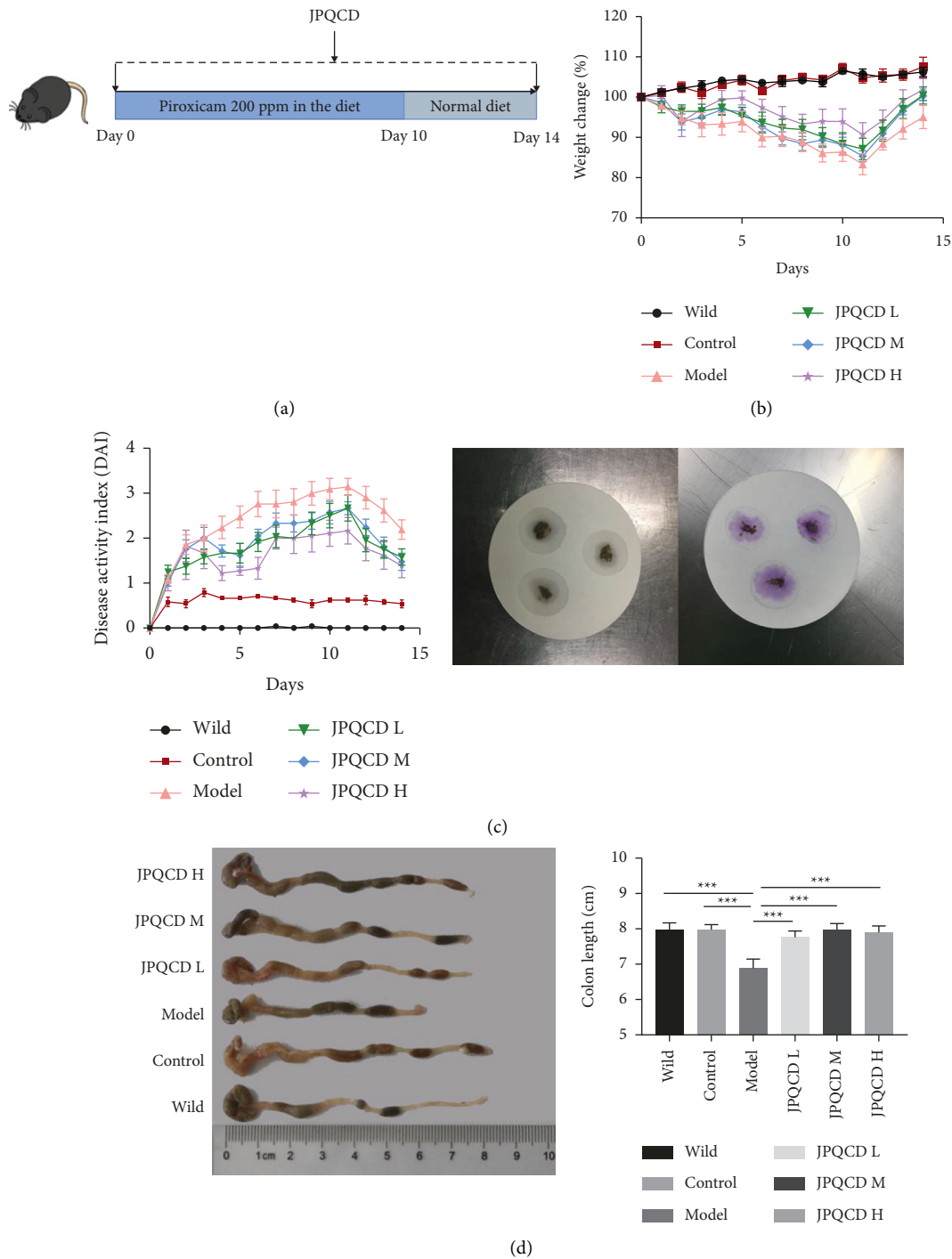


FIGURE 2: JPQCD can improve the symptoms of experimental chronic colitis in *IL-10<sup>-/-</sup>* mice: (a) animal experiment design. *IL-10<sup>-/-</sup>* mice were induced by piroxicam for 10 days. Wild-type/control group/model group and JPQCD group were given normal saline or JPQCD daily. *n* = 6–8. (b) The body weight was measured every day. (c) Schematic diagram of disease activity index score and fecal occult blood test. (d) Colon length and statistics. Data are shown as the mean ± SEM. Compared to the model group, \**P* < 0.05, \*\**P* < 0.01, \*\*\**P* < 0.001.

inflammatory cell infiltration, epithelial hyperplasia, crypt abscess, ulceration, and intestinal wall thickening [22, 23]. Compared with the traditional chemical reagents induction method, this model involves the interaction of genetic factors and immunity and can better simulate the multifactorial human IBD, which is of importance for

exploring the pathogenesis of this disease [24]. In this study, piroxicam was added to the model feed at 200 ppm for 10 d to induce colitis in *IL-10<sup>-/-</sup>* mice, and the mice in the model group showed significant weight loss, thin fecal matter, and positive fecal occult blood test [16]. H&E staining showed that the colonic epithelium of the model

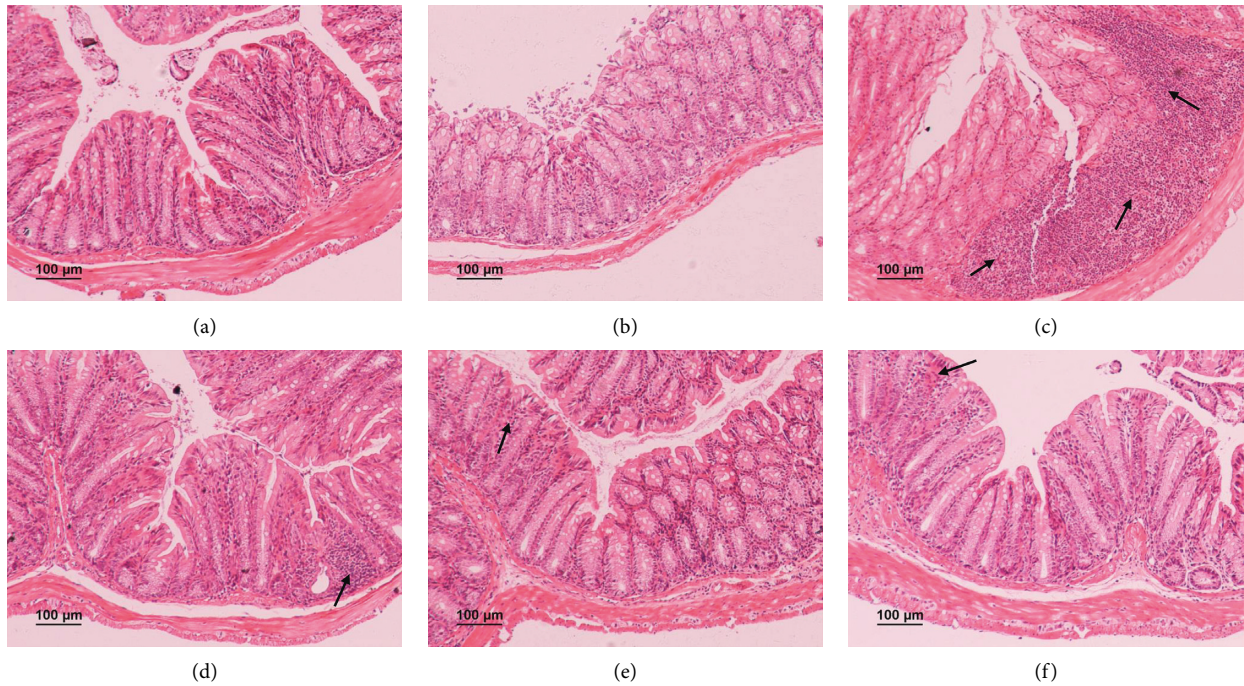


FIGURE 3: Histologic images of mice colon (H&E, magnification  $\times 100$ ). (a) Wild-type group; (b) the control group; (c) model group; (d) low-dose JPQCD group; (e) middle-dose JPQCD group; (f) high-dose JPQCD group. The arrow represents the infiltration of inflammatory cells.

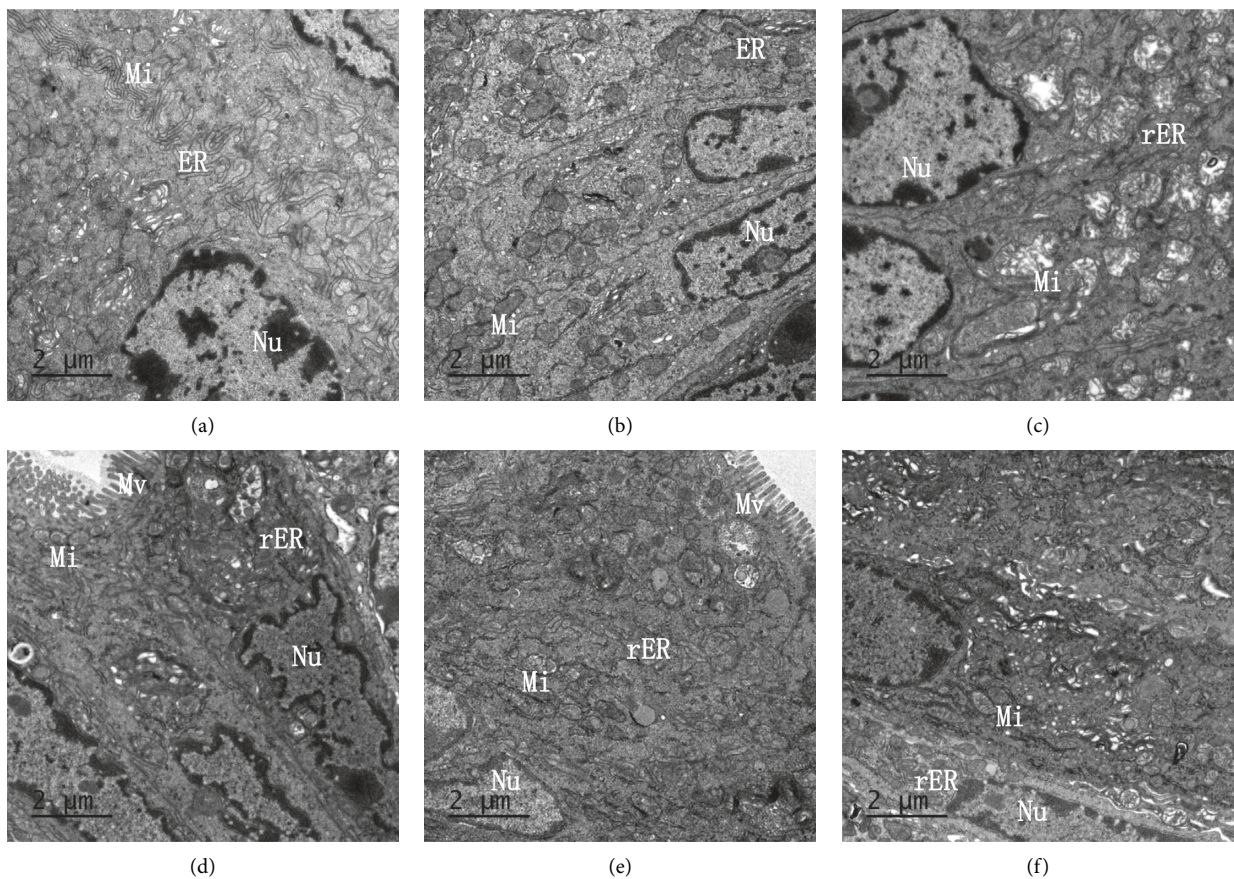


FIGURE 4: Transmission electron microscopy of mouse intestinal epithelial cells (magnification  $\times 6000$ ). (a) Wild-type group; (b) the control group; (c) model group; (d) low-dose JPQCD group; (e) middle-dose JPQCD group; (f) high-dose JPQCD group. Nu: nucleus; Mi: mitochondrial; ER: endoplasmic reticulum; rER: rough endoplasmic reticulum; Mv: microvillus.

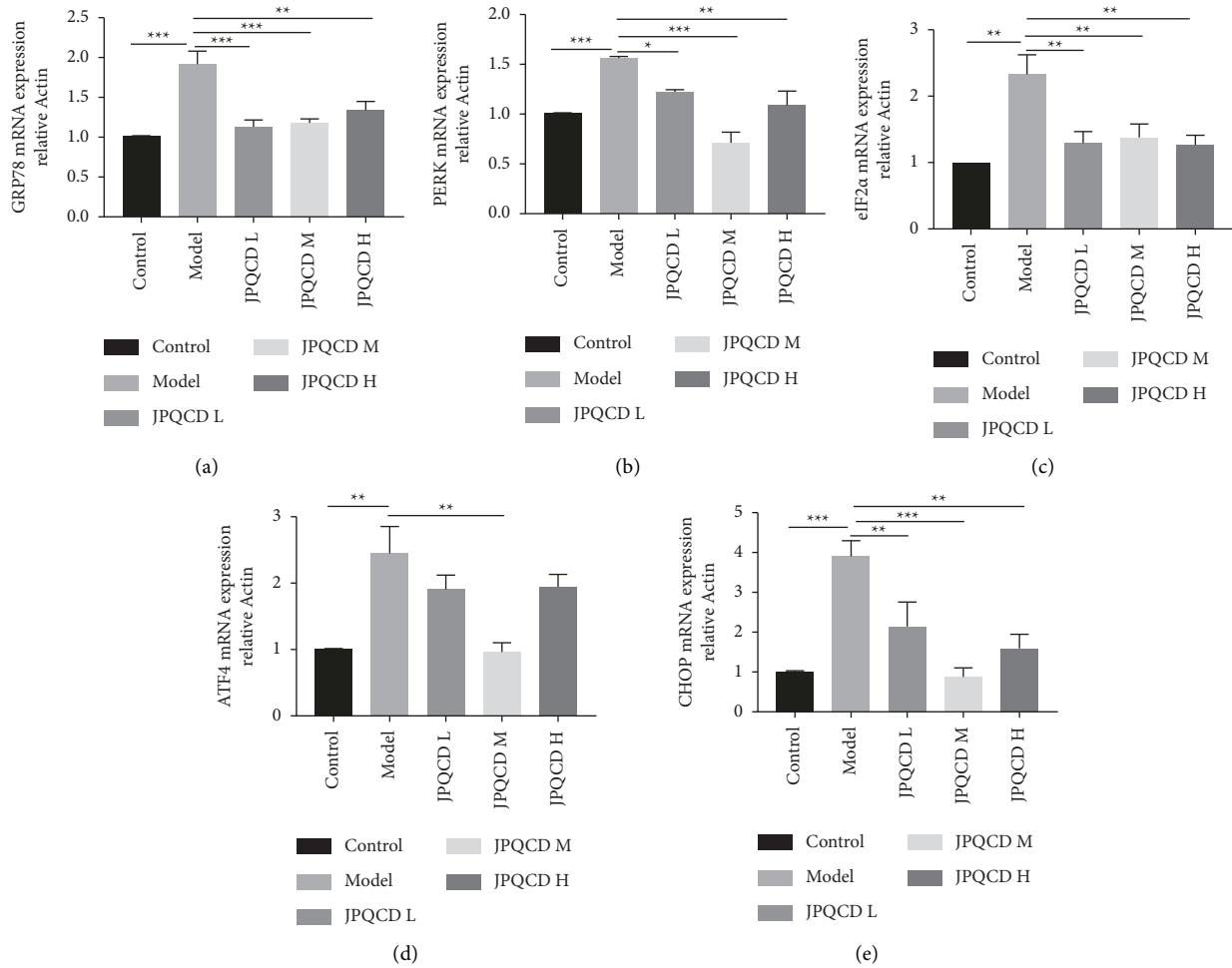


FIGURE 5: Effects of Jianpi Qingchang decoction (JPQCD) on the expression of GRP78, PERK, eIF2 $\alpha$ , ATF4, and CHOP mRNA by RT-PCR in piroxicam-induced colitis *IL-10*<sup>-/-</sup> mice. Data are shown as the mean  $\pm$  SEM. Compared to the model group, \* $P < 0.05$ , \*\* $P < 0.01$ , \*\*\* $P < 0.001$ .

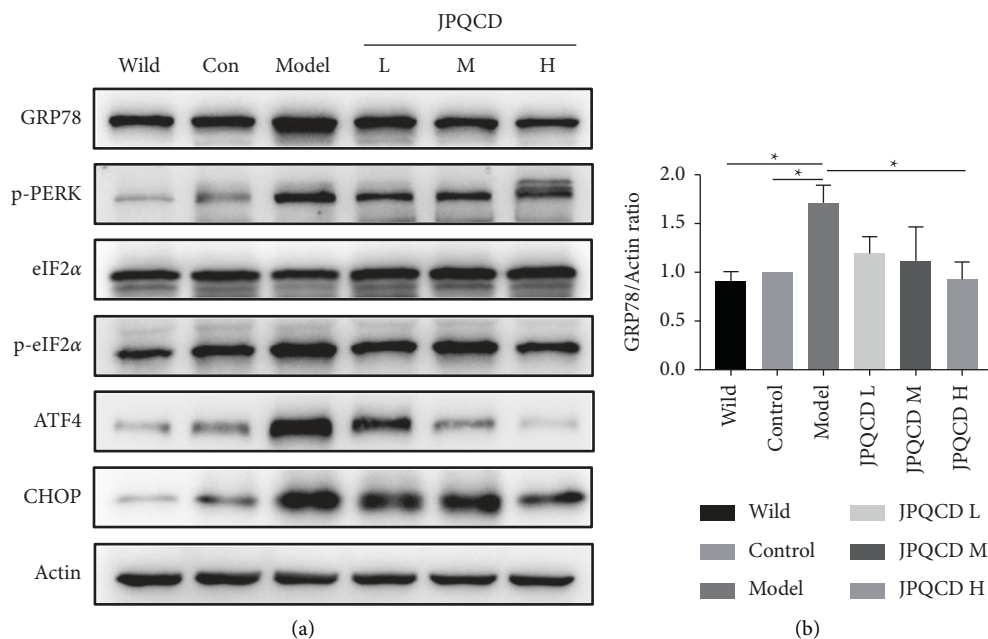
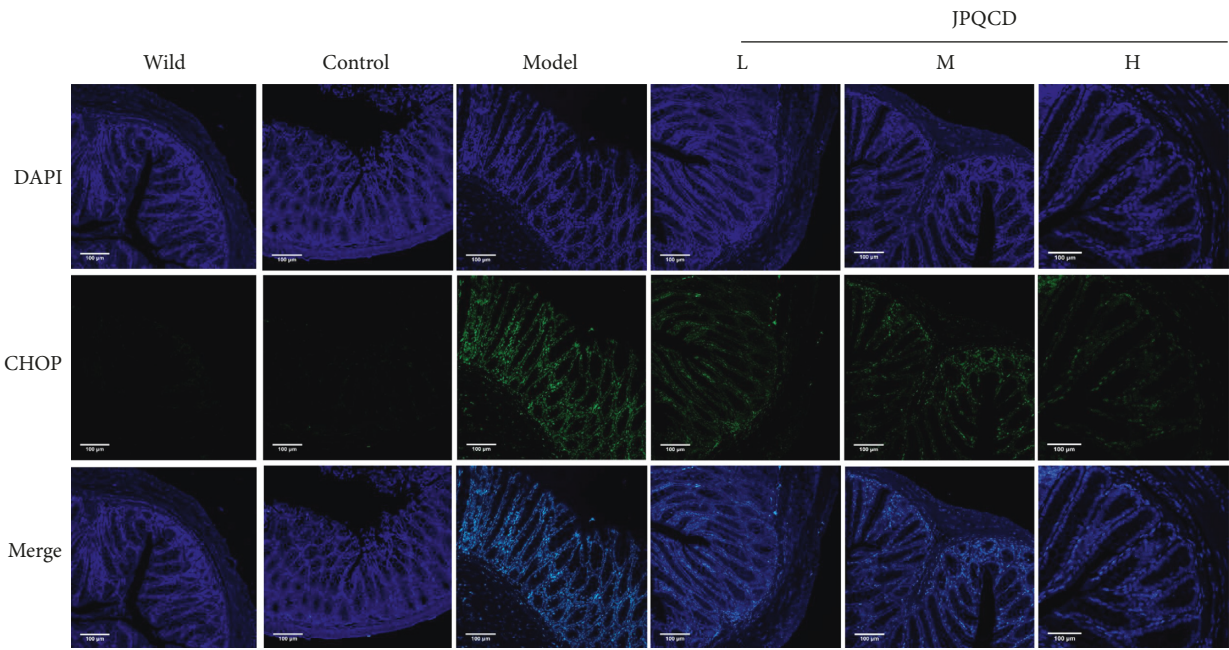
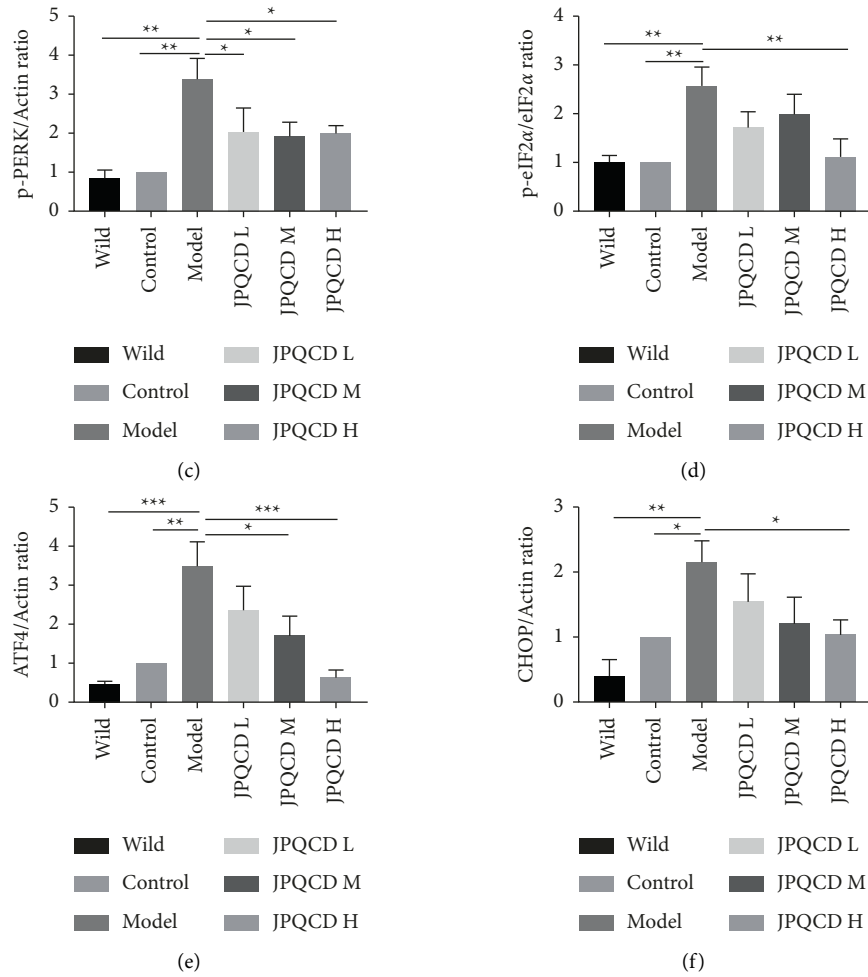


FIGURE 6: Continued.



(g)

FIGURE 6: (a) Effects of Jianpi Qingchang decoction (JPQCD) on the expression of PERK/eIF2α/ATF4/CHOP pathway proteins assessed by western blot in piroxicam-induced colitis *IL-10*<sup>-/-</sup> mice. (b-f) Densitometric analysis was performed to determine each protein. β-Actin was used as the loading control. Data are shown as the mean ± SEM. Compared to the model group, \**P* < 0.05, \*\**P* < 0.01, \*\*\**P* < 0.001. (g) Immunofluorescence staining for CHOP in colon tissues (magnification ×100).

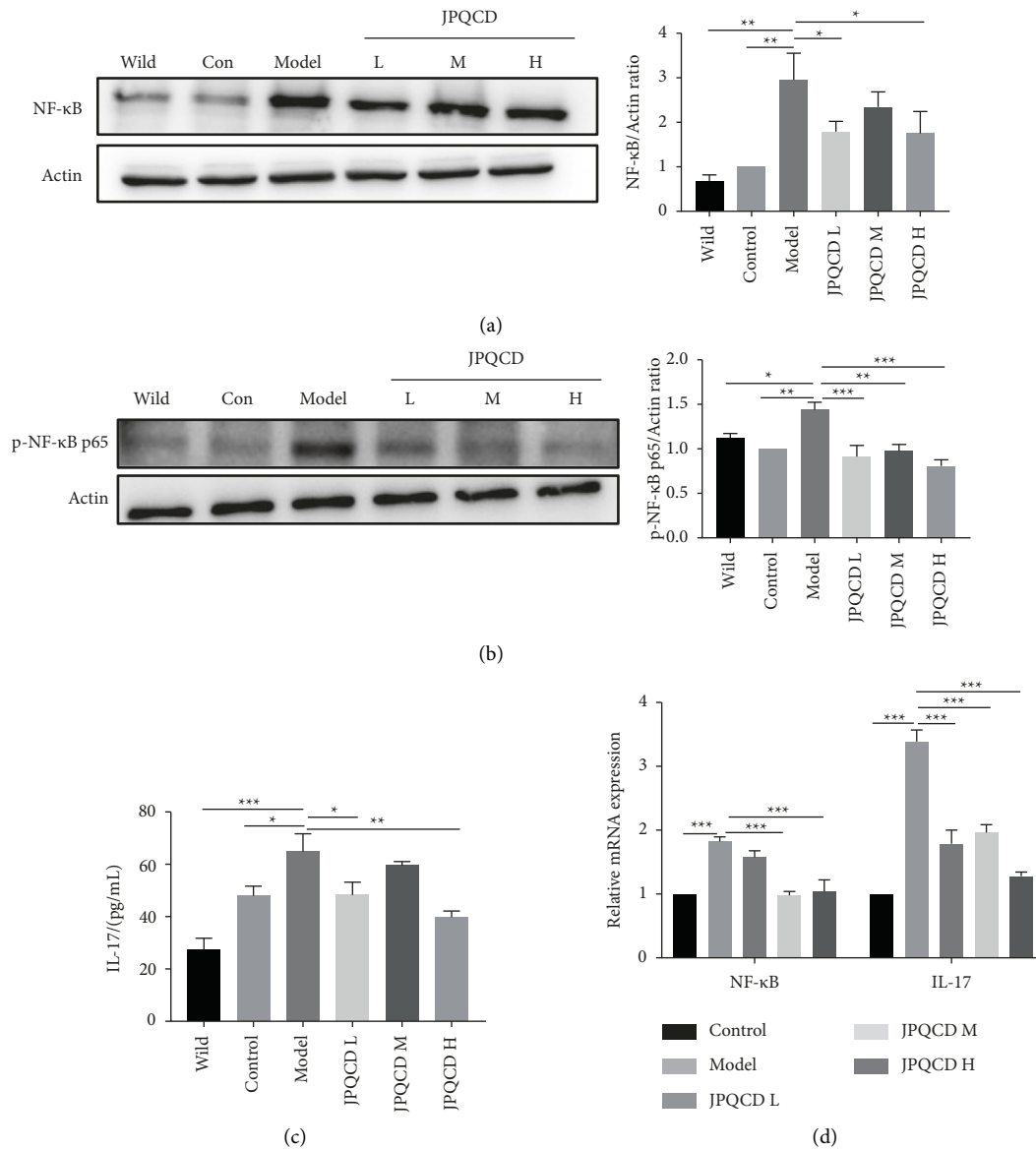


FIGURE 7: (a-b) Western blotting of NF- $\kappa$ B, p-NF- $\kappa$ B p65 in colon tissue. (c) Detection of IL-17 content in colon tissue by ELISA. (d) The mRNA levels of NF- $\kappa$ B and IL-17 in colon tissue. Data are shown as the mean  $\pm$  SEM. Compared to the model group, \* $P < 0.05$ , \*\* $P < 0.01$ , \*\*\* $P < 0.001$ .

group showed obvious ulceration, disordered arrangement of glands, and a large amount of inflammatory cell infiltration, indicating the success of the model.

IEC has an abundant ER structure and is continuously stimulated by intestinal flora, mucosal inflammatory mediators, and other ER stressors [25]. Studies have shown that excessive ER stress in IECs may be involved in the pathogenesis of IBD [26]. Increased expression of ER stress markers has also been observed in colonic epithelial tissues of active IBD patients [27, 28]. Therefore, improving ER stress to restore intestinal homeostasis may be a potential therapeutic target for IBD. The PERK pathway mediated by ER stress plays a key role in the pathological mechanism of UC. When ER stress occurs, PERK is dissociated from GRP78, and the activated PERK phosphorylates eIF2 $\alpha$ ,

which stops most protein synthesis in the cells, reduces the overall protein synthesis level, and increases the selectivity of ATF4 translation [11, 29]. *CHOP* gene is a transcription factor downstream of PERK and a direct target of ATF4, and studies have confirmed that initiation of CHOP is induced by the continuous activation of the PERK pathway [30]. When a severe UPR is caused, ATF4 upregulates *CHOP* gene expression and induces apoptosis. In this study, the phosphorylation of PERK and eIF2 $\alpha$ , the expression of ATF4 and CHOP proteins, and the mRNA expression of PERK, eIF2 $\alpha$ , ATF4, and Chop in the colon tissue of the model group were increased, suggesting that the PERK-eIF2 $\alpha$ -ATF4-CHOP signaling pathway was activated. JPQCD could significantly downregulate the phosphorylation of PERK and eIF2 $\alpha$ , the expression of ATF4 and CHOP proteins, and CHOP mRNA

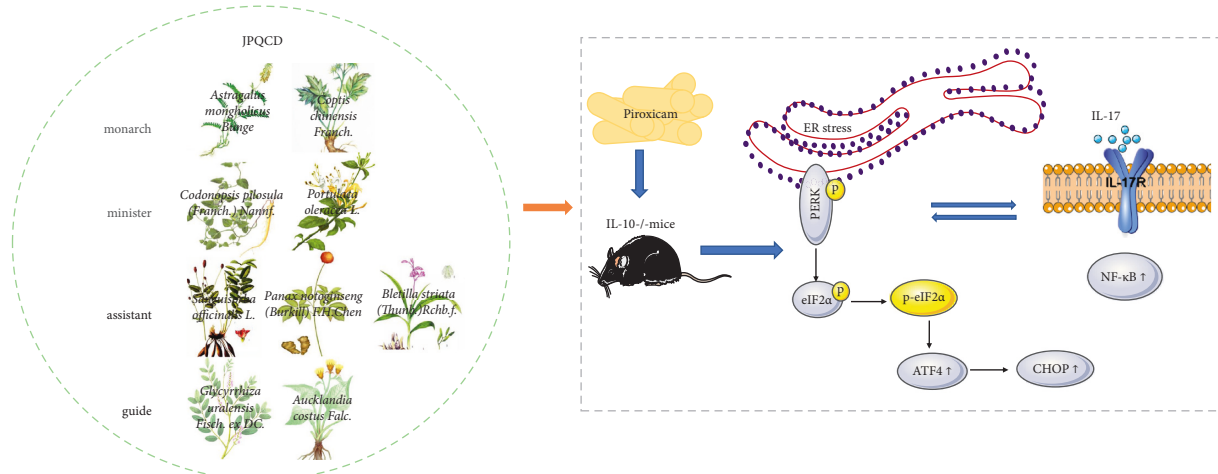


FIGURE 8: Schematic diagram of endoplasmic reticulum stress mechanism of Jianpi Qingchang decoction (JPQCD) in the process of improving piroxicam-induced chronic colitis in  $IL-10^{-/-}$  mice. (Plant illustrations originate from the Internet.)

expression of PERK, eIF2 $\alpha$ , ATF4, and CHOP so as to inhibit intestinal inflammation. Consistent results were obtained with immunofluorescence staining for the apoptotic gene CHOP, and JPQCD significantly reduced the fluorescent expression of CHOP in colonic sections. These results suggest that JPQCD alleviates ER stress and plays an anti-inflammatory role by inhibiting the PERK/eIF2 $\alpha$ /ATF4/CHOP pathway.

The imbalance between proinflammatory and anti-inflammatory cytokines in IBD affects local intestinal inflammation and tissue damage. Blocking these inflammatory mediators is one of the mechanisms that reduce or even reverse the symptoms of IBD [31]. ER stress increases the production of cytokines, including IL-1 $\beta$ , IL-6, IL-8, and TNF- $\alpha$  [32, 33]. Studies have shown that CHOP can induce dendritic cells to secrete IL-23, which may promote the production of IL-17 by local T cells, thus triggering an innate immune response [34]. Under the condition of chronic inflammation, the expression of ER stress marker molecules GRP78 and p-eIF2 $\alpha$  was increased in the intestinal epithelial cells of  $IL-10^{-/-}$  mice [35]. Therefore, we hypothesized that  $IL-10^{-/-}$  mice exposed to piroxicam produced a large number of inflammatory cytokines in the colon and damaged the intestinal mucosa. The barrier function of the intestinal mucosa is damaged, leading to excessive ER stress, causing intestinal inflammation, which in turn promotes cytokine secretion and further aggravates inflammation. IL-17 is a proinflammatory cytokine specifically secreted by helper T cells (Th17). When IL-17 specifically binds to IL-17R on the cell surface, it activates I $\kappa$ B kinase, resulting in the phosphorylation of I $\kappa$ B protein, ubiquitination and degradation, activation of NF- $\kappa$ B signal transduction pathway, and mediation of inflammatory response [36]. Our results showed that the content of IL-17 and mRNA expression in colonic tissue of mice in the model group were significantly increased, confirming that IL-17 was involved in the piroxicam-induced experimental colitis in  $IL-10^{-/-}$  mice, and the intervention of JPQCD could reduce IL-17 level. Previous studies have shown that JPQCD

can reduce DSS-induced acute colitis in mice by inhibiting the activation of NF- $\kappa$ B [14]. In this study, the protein expression of NF- $\kappa$ B, p-NF- $\kappa$ B p65 and mRNA expression of NF- $\kappa$ B in the colon tissues of  $IL-10^{-/-}$  induced by piroxicam were increased, while JPQCD significantly down-regulated the expression of NF- $\kappa$ B.

JPQCD is composed of nine TCMs, each of which contains a variety of compounds, including known anti-UC components, such as berberine, astragalus polysaccharide, and Codonopsis pilosula polysaccharide. Pharmacological studies showed that berberine, the active component of *Coptis chinensis*, could inhibit the Th17 response, protect the colon barrier function of mice, regulate the intestinal flora of mice, and have a significant protective effect on DSS-induced colon injury and inflammation in mice [37–39]. Astragalus polysaccharide can reduce the severity of DSS-induced colitis in mice, and this protective effect may be mediated by inhibiting the activation of NF- $\kappa$ B [40]. *Codonopsis pilosula* polysaccharide and *Codonopsis pilosula* saponin, the main active components of *Codonopsis pilosula*, can synergistically regulate the balance of proinflammatory and anti-inflammatory cytokines, enhance the immune response of the body, and inhibit the colonization of pathogenic bacteria, thereby reducing the symptoms of colitis in UC mice [41]. Polysaccharide from *Scutellaria baicalensis* Georgi can improve colitis by inhibiting the NF- $\kappa$ B signaling pathway and activation of NLRP3 inflammasome [42]. The synergistic effect of various compounds may be key to the role of JPQCD in the treatment of UC. In this study, JPQCD significantly improved UC symptoms, such as weight loss, increased DAI, and improved colonic shortening and colorectal bleeding in  $IL-10^{-/-}$  mice with piroxicam-induced colitis. In addition, JPQCD inhibited crypt epithelial deformation, goblet cell loss, inflammatory cell infiltration, and inflammatory response and alleviated histopathological lesions in the colonic mucosa and submucosa of mice. These results suggest that JPQCD is an ideal natural drug for the prevention and treatment of UC and other IBDs.

In this study, the efficacy of JPQCD did not increase with the dose. In most cases, a medium-dose JPQCD is more effective. Due to the complex components and effects of traditional Chinese medicine and the individual differences of animals and the limited number of samples, there is often no obvious dose-effect relationship in pharmacodynamics tests. The medium dose is the human equivalent dose, which is based on the experience of JPQCD and the experience of famous experts. This animal experiment has well verified the clinical efficacy of the drug.

## 5. Conclusion

In summary, IEC stress induced by piroxicam in *IL-10*<sup>-/-</sup> mice is excessive and activates the PERK/eIF2 $\alpha$ /ATF4/CHOP pathway. JPQCD can reduce ER stress, regulate the PERK/eIF2 $\alpha$ /ATF4/CHOP pathway, repair the intestinal mucosal barrier in mice, and prevent and treat UC.

## Abbreviations

ER:	Endoplasmic reticulum
IEC:	Intestinal epithelial cells
UC:	Ulcerative colitis
JPQCD:	Jianpi Qingchang decoction
RT-PCR:	Reverse transcription-polymerase chain reaction
ELISA:	Enzyme-linked immunosorbent assay
IBD:	Inflammatory bowel disease
TCM:	Traditional Chinese medicine
UPR:	Unfolded protein response
PERK:	Protein kinase-related endoplasmic reticulum kinase
IRE1:	Inositol-requiring enzyme 1
ATF6:	Activating transcription factor 6
GRP78:	Glucose-regulated protein 78
DSS:	Dextran sodium sulfate
NF- $\kappa$ B:	Nuclear factor- $\kappa$ B
IL-1 $\beta$ :	Interleukin-1 $\beta$
DAI:	Disease activity index
H&E:	Hematoxylin and eosin
NSAIDs:	Nonsteroidal anti-inflammatory drugs.

## Data Availability

The datasets generated during and/or analyzed during the current study will be available upon request from the principle investigator. The shared data will only be allowed to be used by the applicant for scientific studies. No commercial activities are allowed.

## Ethical Approval

This study was approved by the Laboratory Animal Ethics Committee of Shanghai University of Chinese Medicine (PZSHUTCM190912020).

## Consent

All participants signed informed consent.

## Disclosure

Chen Q and Zhang YL are co-first authors.

## Conflicts of Interest

The authors declare that there are no conflicts of interest related to this work.

## Authors' Contributions

Chen Q and Zhang YL contributed equally and finished the major experiments; Dai YC performed the experiments and analyzed the data; Zhang ZW, Chen YJ, and Tang YJ participated in the treatment of animals; Qiao D supplemented some molecular experiments. Tang ZP designed and coordinated the research; all authors read and approved the final manuscript. Qian Chen and Ya-Li Zhang contributed equally to this work.

## Acknowledgments

This study was supported by the National Natural Science Foundation of China, Nos. 81573892, 81873253, and 81704009; Key Clinical Specialty Construction Project Supported by Hongkou District Health Committee, No. HKZK2020A01; Xinglin Scholar Program of Shanghai University of Traditional Chinese Medicine; the document of the Shanghai University of Traditional Chinese Medicine 2020, No. 23; and Shanghai University of Traditional Chinese Medicine Budget Project, No. 2021LK041.

## References

- [1] R. Ungaro, S. Mehandru, P. B. Allen, L. Peyrin-Biroulet, and J.-F. Colombel, "Ulcerative colitis," *The Lancet*, vol. 389, no. 10080, pp. 1756–1770, 2017.
- [2] K. Nanki, M. Fujii, M. Shimokawa et al., "Somatic inflammatory gene mutations in human ulcerative colitis epithelium," *Nature*, vol. 577, no. 7789, pp. 254–259, 2019.
- [3] K. Yeshi, R. Ruscher, L. Hunter, N. L. Daly, A. Loukas, and P. Wangchuk, "Revisiting inflammatory bowel disease: pathology, treatments, challenges and emerging therapeutics including drug leads from natural products," *Journal of Clinical Medicine*, vol. 9, no. 5, p. 1273, 2020.
- [4] B.-J. Guo, Z.-X. Bian, H.-C. Qiu, Y.-T. Wang, and Y. Wang, "Biological and clinical implications of herbal medicine and natural products for the treatment of inflammatory bowel disease," *Annals of the New York Academy of Sciences*, vol. 1401, no. 1, pp. 37–48, 2017.
- [5] G. Holleran, F. Scaldaferrri, A. Gasbarrini, and D. Currò, "Herbal medicinal products for inflammatory bowel disease: a focus on those assessed in double-blind randomised controlled trials," *Phytotherapy Research*, vol. 34, no. 1, pp. 77–93, 2019.
- [6] M. Abdullah, A. F. Syam, M. Simadibrata, J. Gunawan, D. Makmun, and A. A. Rani, "New insights on the pathomechanisms of inflammatory bowel disease," *Journal of Digestive Diseases*, vol. 14, no. 9, pp. 455–462, 2013.
- [7] S. Hosomi, A. Kaser, and R. S. Blumberg, "Role of endoplasmic reticulum stress and autophagy as interlinking pathways in the pathogenesis of inflammatory bowel disease,"

- Current Opinion in Gastroenterology*, vol. 31, no. 1, pp. 81–88, 2015.
- [8] K. Luo and S. S. Cao, “Endoplasmic reticulum stress in intestinal epithelial cell function and inflammatory bowel disease,” *Gastroenterology Research and Practice*, vol. 2015, Article ID 328791, 6 pages, 2015.
  - [9] A. Almanza, A. Carlesso, C. Chintha et al., “Endoplasmic reticulum stress signalling—from basic mechanisms to clinical applications,” *FEBS Journal*, vol. 286, no. 2, pp. 241–278, 2019.
  - [10] X. Ma, Z. Dai, K. Sun et al., “Intestinal epithelial cell endoplasmic reticulum stress and inflammatory bowel disease pathogenesis: an update review,” *Frontiers in Immunology*, vol. 8, 2017.
  - [11] H. P. Harding, Y. Zhang, A. Bertolotti, H. Zeng, and D. Ron, “Perk is essential for translational regulation and cell survival during the unfolded protein response,” *Molecular Cell*, vol. 5, no. 5, pp. 897–904, 2000.
  - [12] Y.-C. Dai, L. Zheng, Y.-L. Zhang, X. Chen, D.-L. Chen, and Z.-P. Tang, “Effects of Jianpi Qingchang decoction on the quality of life of patients with ulcerative colitis,” *Medicine*, vol. 96, no. 16, Article ID e6651, 2017.
  - [13] Y.-L. Chen, Y.-Y. Zheng, Y.-C. Dai, Y.-L. Zhang, and Z.-P. Tang, “Systems pharmacology approach reveals protective mechanisms of Jian-Pi Qing-Chang decoction on ulcerative colitis,” *World Journal of Gastroenterology*, vol. 25, no. 21, pp. 2603–2622, 2019.
  - [14] L. Zheng, Y.-L. Zhang, Y.-C. Dai et al., “Jianpi Qingchang decoction alleviates ulcerative colitis by inhibiting nuclear factor- $\kappa$ B activation,” *World Journal of Gastroenterology*, vol. 23, no. 7, pp. 1180–1188, 2017.
  - [15] Y.-C. Dai, L. Zheng, Y.-L. Zhang et al., “Jianpi Qingchang decoction regulates intestinal motility of dextran sulfate sodium-induced colitis through reducing autophagy of interstitial cells of Cajal,” *World Journal of Gastroenterology*, vol. 23, no. 26, pp. 4724–4734, 2017.
  - [16] S.-J. Koh, J. W. Kim, B. G. Kim, K. L. Lee, J. Chun, and J. S. Kim, “Fexofenadine regulates nuclear factor- $\kappa$ B signaling and endoplasmic reticulum stress in intestinal epithelial cells and ameliorates acute and chronic colitis in mice,” *Journal of Pharmacology and Experimental Therapeutics*, vol. 352, no. 3, pp. 455–461, 2015.
  - [17] S. Sánchez-Fidalgo, A. Cárdeno, M. Sánchez-Hidalgo, M. Aparicio-Soto, and C. A. de la Lastra, “Dietary extra virgin olive oil polyphenols supplementation modulates DSS-induced chronic colitis in mice,” *The Journal of Nutritional Biochemistry*, vol. 24, no. 7, pp. 1401–1413, 2013.
  - [18] R. Kühn, J. Löhler, D. Rennick, K. Rajewsky, and W. Müller, “Interleukin-10-deficient mice develop chronic enterocolitis,” *Cell*, vol. 75, no. 2, pp. 263–274, 1993.
  - [19] E. Mizoguchi, D. Low, Y. Ezaki, and T. Okada, “Recent updates on the basic mechanisms and pathogenesis of inflammatory bowel diseases in experimental animal models,” *Intestinal Research*, vol. 18, no. 2, pp. 151–167, 2020.
  - [20] H. Wang, J. G. Vilches-Moure, S. Cherkaoui et al., “Chronic model of inflammatory bowel disease in IL-10 $^{-/-}$  transgenic mice: evaluation with ultrasound molecular imaging,” *Theranostics*, vol. 9, no. 21, pp. 6031–6046, 2019.
  - [21] M. Xie, H. Zhang, W. Wang et al., “Tricloroan exposure exaggerates spontaneous colonic inflammation in il-10 $^{-/-}$  mice,” *Toxicological Sciences*, vol. 174, no. 1, pp. 92–99, 2020.
  - [22] L. P. Hale and P. K. Greer, “A novel murine model of inflammatory bowel disease and inflammation-associated colon cancer with ulcerative colitis-like features,” *PLoS One*, vol. 7, no. 7, Article ID e41797, 2012.
  - [23] Y. L. Jones-Hall and M. B. Grisham, “Immunopathological characterization of selected mouse models of inflammatory bowel disease: comparison to human disease,” *Pathophysiology*, vol. 21, no. 4, pp. 267–288, 2014.
  - [24] L. M. Keubler, M. Buettner, C. Häger, and A. Bleich, “A multihit model,” *Inflammatory Bowel Diseases*, vol. 21, no. 8, pp. 1967–1975, 2015.
  - [25] M. A. McGuckin, R. D. Eri, I. Das, R. Lourie, and T. H. Florin, “ER stress and the unfolded protein response in intestinal inflammation,” *American Journal of Physiology-Gastrointestinal and Liver Physiology*, vol. 298, no. 6, pp. G820–G832, 2010.
  - [26] S. S. Cao, E. M. Zimmermann, B. M. Chuang et al., “The unfolded protein response and chemical chaperones reduce protein misfolding and colitis in mice,” *Gastroenterology*, vol. 144, no. 5, pp. 989–1000, Article ID e1006, 2013.
  - [27] S. Bogaert, M. De Vos, K. Olivevier et al., “Involvement of endoplasmic reticulum stress in inflammatory bowel disease: a different implication for colonic and ileal disease?” *PLoS One*, vol. 6, no. 10, Article ID e25589, 2011.
  - [28] A. Kaser, A.-H. Lee, A. Franke et al., “XBP1 links ER stress to intestinal inflammation and confers genetic risk for human inflammatory bowel disease,” *Cell*, vol. 134, no. 5, pp. 743–756, 2008.
  - [29] B. B. Rasmussen and C. M. Adams, “ATF4 is a fundamental regulator of nutrient sensing and protein turnover,” *Journal of Nutrition*, vol. 150, no. 5, pp. 979–980, 2020.
  - [30] H. Zinszner, M. Kuroda, X. Wang et al., “CHOP is implicated in programmed cell death in response to impaired function of the endoplasmic reticulum,” *Genes & Development*, vol. 12, no. 7, pp. 982–995, 1998.
  - [31] U. P. Singh, N. P. Singh, E. A. Murphy et al., “Chemokine and cytokine levels in inflammatory bowel disease patients,” *Cytokine*, vol. 77, pp. 44–49, 2016.
  - [32] K. Shenderov, N. Riteau, R. Yip et al., “Cutting edge: endoplasmic reticulum stress licenses macrophages to produce mature IL-1 $\beta$  in response to TLR4 stimulation through a caspase-8- and TRIF-dependent pathway,” *The Journal of Immunology (Baltimore, Md: 1950)*, vol. 192, no. 5, pp. 2029–2033, 2014.
  - [33] A. K. Ghosh, S. K. Garg, T. Mau, M. O’Brien, J. Liu, and R. Yung, “Elevated endoplasmic reticulum stress response contributes to adipose tissue inflammation in aging,” *The Journals of Gerontology Series A: Biological Sciences and Medical Sciences*, vol. 70, no. 11, pp. 1320–1329, 2015.
  - [34] J. C. Goodall, C. Wu, Y. Zhang et al., “Endoplasmic reticulum stress-induced transcription factor, CHOP, is crucial for dendritic cell IL-23 expression,” *Proceedings of the National Academy of Sciences*, vol. 107, no. 41, pp. 17698–17703, 2010.
  - [35] A. Shkoda, P. A. Ruiz, H. Daniel et al., “Interleukin-10 blocked endoplasmic reticulum stress in intestinal epithelial cells: impact on chronic inflammation,” *Gastroenterology*, vol. 132, no. 1, pp. 190–207, 2007.
  - [36] S. Zhu and Y. Qian, “IL-17/IL-17 receptor system in autoimmune disease: mechanisms and therapeutic potential,” *Clinical Science: (1979)*, vol. 122, no. 11, pp. 487–511, 2012.
  - [37] Y.-h. Li, H.-t. Xiao, D.-d. Hu et al., “Berberine ameliorates chronic relapsing dextran sulfate sodium-induced colitis in C57BL/6 mice by suppressing Th17 responses,” *Pharmacological Research*, vol. 110, pp. 227–239, 2016.
  - [38] Y. Liu, X. Liu, W. Hua et al., “Berberine inhibits macrophage M1 polarization via AKT1/SOCS1/NF- $\kappa$ B signaling pathway to protect against DSS-induced colitis,” *International Immunopharmacology*, vol. 57, pp. 121–131, 2018.

- [39] H. Cui, Y. Cai, L. Wang et al., “Berberine regulates treg/Th17 balance to treat ulcerative colitis through modulating the gut microbiota in the colon,” *Frontiers in Pharmacology*, vol. 9, p. 571, 2018.
- [40] J. Lv, Y. Zhang, Z. Tian et al., “Astragalus polysaccharides protect against dextran sulfate sodium-induced colitis by inhibiting NF- $\kappa$ B activation,” *International Journal of Biological Macromolecules*, vol. 98, pp. 723–729, 2017.
- [41] Y. Jing, A. Li, Z. Liu et al., “Absorption of Codonopsis pilosula saponins by coexisting polysaccharides alleviates gut microbial dysbiosis with dextran sulfate sodium-induced colitis in model mice,” *BioMed Research International*, vol. 2018, Article ID 1781036, 18 pages, 2018.
- [42] L. Cui, W. Wang, Y. Luo et al., “Polysaccharide from *Scutellaria baicalensis* Georgi ameliorates colitis via suppressing NF- $\kappa$ B signaling and NLRP3 inflammasome activation,” *International Journal of Biological Macromolecules*, vol. 132, pp. 393–405, 2019.